How does colored dissolved organic matter (CDOM) influence the distribution and intensity of hypoxia in coastal oceans?

Rui Jin[1], Anand Gnanadesikan[1], Marie-Aude Sabine Pradal[1], and Pierre St-Laurent[2]

[1]Johns Hopkins University
[2]Virginia Institute of Marine Science (VIMS)

September 30, 2023

Abstract

Excessive nutrient loading is a well-established driver of hypoxia in aquatic ecosystems. However, recent limnological research has illuminated the role of Chromophoric Dissolved Organic Matter (CDOM) in exacerbating hypoxic conditions, particularly in freshwater lakes. In coastal ocean environments, the influence of CDOM on hypoxia remains an underexplored area of investigation. This study seeks to elucidate the intricate relationship between CDOM and hypoxia by employing a nitrogen-based model within the context of Chesapeake Bay, a large estuary with unique characteristics including salinity stratification and the localization of hypoxia/anoxia in a 30-meter-deep channel aligned with the estuary's primary stem. Our findings indicate that the impact of CDOM on nutrient dynamics and productivity varies significantly across different regions of Chesapeake Bay. In the upper Bay, the removal of CDOM reduces light limitation, thus promoting increased productivity, resulting in the generation of more detritus and burial, which, in turn, contributes to elevated levels of hypoxia. As we transition to the middle and lower Bay, the removal of CDOM can cause a decline in integrated primary productivity due to nutrient uptake in the upper Bay. This decrease in productivity is associated with reduced burial and denitrification, ultimately leading to a decrease in hypoxia levels. Streamflow modulates this impact. The time integral of the hypoxic volume during low-flow years is particularly sensitive to CDOM removal, while in high-flow years, it is relatively unchanged. This research underscores the necessity for a comprehensive understanding of the intricate interactions between CDOM and hypoxia in coastal ecosystems.

Hosted file

`973483_0_art_file_11407657_s1b5vd.docx` available at https://authorea.com/users/535090/articles/667774-how-does-colored-dissolved-organic-matter-cdom-influence-the-distribution-and-intensity-of-hypoxia-in-coastal-oceans

How Does Colored Dissolved Organic Matter (CDOM) Influence the Distribution and Intensity of Hypoxia in Coastal Oceans?

Rui Jin[1], Anand Gnanadesikan[1], Marie-Aude Pradal[1] and Pierre St-Laurent[2]

[1] Department of Earth and Planetary Sciences, Johns Hopkins University, Baltimore, Maryland, USA

[2] Virginia Institute of Marine Science, William & Mary, Gloucester Point, Virginia, USA

Corresponding author: Rui Jin (ruijin@jhu.edu)

Key Points:

- Colored dissolved organic matter can impact hypoxia within Chesapeake Bay by changing the absorption of light.
- In the upper Bay, removing CDOM alleviates light limitation, stimulates primary productivity and increases hypoxia, but also burial.
- In the middle and lower Bay, CDOM removal reduces integrated primary productivity and hypoxia due to nutrient uptake in the upper Bay.

Abstract

Excessive nutrient loading is a well-established driver of hypoxia in aquatic ecosystems. However, recent limnological research has illuminated the role of Chromophoric Dissolved Organic Matter (CDOM) in exacerbating hypoxic conditions, particularly in freshwater lakes. In coastal ocean environments, the influence of CDOM on hypoxia remains an underexplored area of investigation. This study seeks to elucidate the intricate relationship between CDOM and hypoxia by employing a nitrogen-based model within the context of Chesapeake Bay, a large estuary with unique characteristics including salinity stratification and the localization of hypoxia/anoxia in a 30-meter-deep channel aligned with the estuary's primary stem. Our findings indicate that the impact of CDOM on nutrient dynamics and productivity varies significantly across different regions of Chesapeake Bay. In the upper Bay, the removal of CDOM reduces light limitation, thus promoting increased productivity, resulting in the generation of more detritus and burial, which, in turn, contributes to elevated levels of hypoxia. As we transition to the middle and lower Bay, the removal of CDOM can cause a decline in integrated primary productivity due to nutrient uptake in the upper Bay. This decrease in productivity is associated with reduced burial and denitrification, ultimately leading to a decrease in hypoxia levels. Streamflow modulates this impact. The time integral of the hypoxic volume during low-flow years is particularly sensitive to CDOM removal, while in high-flow years, it is relatively unchanged. This research underscores the necessity for a comprehensive understanding of the intricate interactions between CDOM and hypoxia in coastal ecosystems.

Plain Language Summary

Too many nutrients in water can cause a problem called hypoxia, where there is not enough oxygen for aquatic life. Scientists have recently discovered that a substance called Chromophoric Dissolved Organic Matter (CDOM) can make this problem worse, especially in lakes. But when it comes to the coastal ocean, it is not clear that how CDOM affects hypoxia. This study tried to figure out how CDOM and hypoxia are related in Chesapeake Bay, a large inlet with some unique features. We found that CDOM affects nutrient levels and how much life can grow in different parts of the bay. We remove that part of CDOM associated with “refractory” dissolved organic carbon delivered by rivers. The impact on hypoxia is different in various parts of the bay. In regions in and near rivers removing CDOM promotes light penetration and causes more particles to sink to the bottom because of increased productivity thus leads to more hypoxia. However, because nutrients cannot escape, this would in turn lower overall productivity in middle and lower Bay, which results in less burial and less hypoxia in this region. Different amounts of flow will also cause year-to-year variability in hypoxic volume.

1 Introduction

Coastal regions around the world are facing an increasing concern with the emergence of "dead zones" in the ocean. These areas suffer from critically low oxygen levels, below 60-80 μM, which are necessary for the survival of organisms like crabs and shrimp (Diaz and Rosenberg, 2008). The frequency of reported dead zones has doubled every decade since the 1960s, occurring when the supply of oxygen from mixing and circulation fails to meet the demand caused by the decomposition of organic matter. The growing occurrence of dead zones is often attributed to an elevated oxygen demand, which in turn is linked to an increased supply of

nutrients to coastal waters as a result of intensified human activities since World War II, commonly referred to as the "Great Acceleration" (Steffen et al., 2007; Rabalais et al., 2009; Fennel and Testa, 2019). Hypoxia in these zones has significant implications for fisheries, as it limits available habitats, disrupts food webs, diverts primary production, and occasionally leads to large-scale fish mortality events (Luther and Church, 1988; Kemp et al., 2005).

One particular ecosystem of great importance in this context is Chesapeake Bay, the largest estuary in continental North America. It serves as a crucial habitat supporting highly productive fisheries for crabs and oysters, while also playing a vital role as a recreational resource (Brown et al., 2012). Physically, the Bay experiences an inflow of dense, salty Atlantic Water, which gradually mixes and dilutes as it moves northwards through the channel, with the Susquehanna River being the most significant contributor at the head of the Bay. During the summer season, reduced winds lead to strong stratification within the Bay. The presence of hypoxia, characterized by low oxygen levels, was first identified in Chesapeake Bay in 1930 (Kemp et al., 2005) and has shown a substantial increase over time. Since 2015, the maximum estimated hypoxic volume in the Bay, determined by the Virginia Institute of Marine Science (VIMS 2023), has ranged from 6.8 to 17 km^3, accounting for approximately 8 to 21% of the total volume of the Bay. Fluctuations in wind-driven mixing and the riverine nitrogen loading (Scavia et al., 2006) are regarded as major drivers of the variability of hypoxic conditions within the Bay. Understanding and addressing the factors contributing to hypoxia in Chesapeake Bay are crucial for the conservation and management of this ecologically significant estuarine system.

While nutrients and sediments are recognized as crucial factors in the degradation of coastal water quality, it is widely acknowledged that they do not provide a complete explanation for the clarity of coastal waters. Additional factors, such as the presence of natural water compounds, significantly contribute to this phenomenon. Chromophoric or colored dissolved organic matter (CDOM) is a collective term for compounds like humic, protein-like, and pigment-like substances that have a preference for absorbing light on the blue end of the spectrum (Green and Blough, 1994). CDOM is known for its significant refractory nature (Yamashita and Tanoue, 2008), although it gradually degrades through photobleaching processes (Yamashita et al., 2013). CDOM produces substantial levels of light absorption in open-ocean waters (Siegel et al., 2005) and may exert a dominant influence on absorption in coastal waters, including Chesapeake Bay (Cao et al., 2018, Fig. 1). Figure 1 demonstrates that the rivers serve as significant sources of CDOM, resulting in elevated absorption coefficients as one moves up the estuary. The absorption coefficient exhibits a gradual decline as one progresses towards the main stem of the Bay. However even within the central region of the Bay, a substantial absorption coefficient of approximately 4 m^{-1} is observed (Miller et al 2002). Generally, the absorption coefficient for CDOM at 300nm is a factor of ~5 larger than that of Photosynthetically Active Radiation (PAR) absorption, which is dominated by longer wavelengths.

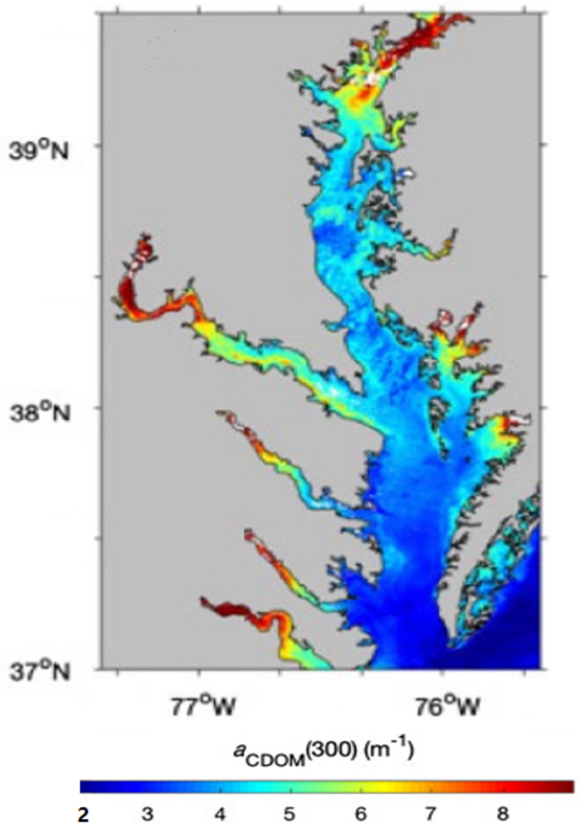

Figure 1: Recent retrieval of CDOM (represented in terms of the absorption coefficient at 300nm wavelength) from the MERIS high-resolution satellite dataset, reported by Cao et al. (2018).

The phenomenon of increased CDOM in lakes, referred to as surface water "browning" or "brownification," has been extensively studied in the field of limnology. This occurrence has been observed to rise in various boreal ecosystems, particularly in glaciated acid-sensitive terrains in Scandinavia, the British Isles, and regions of New York, New England, and Canada (Monteith et al., 2007). Downstream effects on coastal waters have been documented in Norwegian fjords (Aksnes et al., 2009) and the Gulf of Maine (Balch et al., 2016). Additionally, there is emerging evidence suggesting that climate change is accelerating the process of brownification in North America (de Wit et al., 2021). Scientific communities focused on enhancing water quality in rivers, streams, and lakes have begun to recognize the potential impact of managing dissolved organic carbon (DOC) in mitigating brownification (Stanley et al., 2012; Kritzberg et al., 2020; Cao et al., 2020). Efforts to improve water quality near peatland drainage systems, for example, have investigated the effects of ditch density and iron concentration (Estlander et al., 2021). In China, strategies to control "black blooms" (where hypoxia progresses to euxinia) have involved aeration, dredging, and the construction of artificial wetlands (Cao et al., 2020).

CDOM has been found to affect both physical and biogeochemical cycling in many regions. Limnologists have found that increased CDOM in lakes can lead to increased hypoxia, either through reduced benthic primary productivity (Brothers et al., 2014) or increasing stability (Knoll et al., 2018). Changes in ocean color due to CDOM have been observed in the Gulf of

Maine and certain areas of the Baltic Sea (Balch et al., 2016; Kahru et al., 2022). Removing CDOM has been found to increase productivity in the upper water column, leading to elevated surface nutrients, biomass, and chlorophyll, albeit with lower integrated biomass throughout the water column (Kim et al., 2015). Furthermore, the trapping of solar radiation near the surface by CDOM amplifies the seasonal temperature cycle (Gnanadesikan et al., 2019), resulting in warmer summers and colder winters. Consequently, increasing trends in CDOM could potentially contribute to the occurrence of marine heatwaves. In the Arctic region, characterized by high CDOM levels, these temperature changes are mitigated by the annual sea ice cycle, resulting in increased sea ice concentration (Kim et al., 2016). Previous research (Gallegos, 2001) has examined the influence of CDOM on optical properties in Chesapeake Bay. However, the parameterization approach used to characterize CDOM absorption in these studies did not explicitly incorporate CDOM. Instead the effect of CDOM on absorption is implicitly modeled by fitting observed light attenuation to hydrographic parameters (generally total suspended solids and salinity as in Cerco and Noel, 2017). However this makes it difficult to explicitly model the impact of changing CDOM inputs to the Bay.

Although current models exhibit some skill in simulating coastal environments, the representation of CDOM absorption remains rudimentary. This is particularly true for one of the leading models of Chesapeake Bay (Chesroms_ECB, Feng et al., 2015), which represents the impacts of CDOM in terms of salinity-dependent absorption. While this approach is sensible for simulating the current state of the Bay considering the limited knowledge of CDOM dynamics, a more explicit representation of CDOM/Chl absorption has been shown to improve physical simulations (Kim et al., 2020). However, the standard version of Chesroms_ECB basically assumes that the impacts of CDOM absorption can be captured by using salinity. This restricts our ability to examine its separate impact on water clarity and quality. In this study, we aimed to provide a more accurate representation of CDOM absorption in Chesapeake Bay. We also conducted a series of experiments to investigate the dynamics between CDOM and coastal ocean hypoxia.

2 Methods

2.1 Physical model

The model utilized in this study is derived from the Chesroms_ECB model, which was developed and described in Da et al. (2018). The coupled physical-biogeochemical models employed in this work were created using the Regional Ocean Modeling System (ROMS). The physical circulations of the models are based on ROMS revision 898, a three-dimensional, time-dependent simulation utilizing hydrostatic primitive equations (Shchepetkin and McWilliams, 2005) as described in Da et al. (2018). The following description closely follows that from these manuscripts as well as two recent papers (Jin et al., 2023a,b).

The model domain covers the region from 77.2°W to 75.0°W and from 36°N to 40°N, encompassing the main stem and primary tributaries of the Chesapeake Bay. To prevent contamination of tracers and mean velocities by boundary effects, the model extends seaward to the mid-Atlantic Bight. The horizontal grid consists of orthogonal curvilinear coordinates, with

the highest resolution (430m) in the northern Bay, the lowest resolution (approximately 10 km) in the southern end of the mid-Atlantic Bight, and an average grid spacing of 1.7 km within the Chesapeake Bay. The governing equations are discretized using a stretched terrain-following s-coordinate system with 20 vertical levels. To account for varying resolutions between the surface and bottom boundary layers in deep waters and maintain relatively constant resolution in shallow waters, the standard stretching function in ROMS was employed with values of θs=6.0 and θb=4.0 (standard values in this version of ROMS), along with a minimum grid cell thickness hc=10m.

Tidal constituents were adopted from the Advanced Circulation (ADCIRC) model (Leuttich et al., 1992), and observed nontidal water levels from Duck, NC, and Lewes, DE (Scully, 2016), were imposed on the model at the open boundary. Atmospheric forcing, including winds, air temperature, relative humidity, pressure, precipitation, short-wave radiation, and longwave radiation, was obtained from the North American Regional Reanalysis (Mesinger et al., 2006). The MPDATA 3-D advection scheme was employed for tracers, a third-order upstream advection scheme for 3-D horizontal momentum, and a fourth-order centered difference scheme for 3-D momentum in the vertical. The vertical turbulent mixing scheme and background mixing coefficients for both momentum and tracers were all set to the same values as in Feng et al. (2015).

2.2 Biological cycling

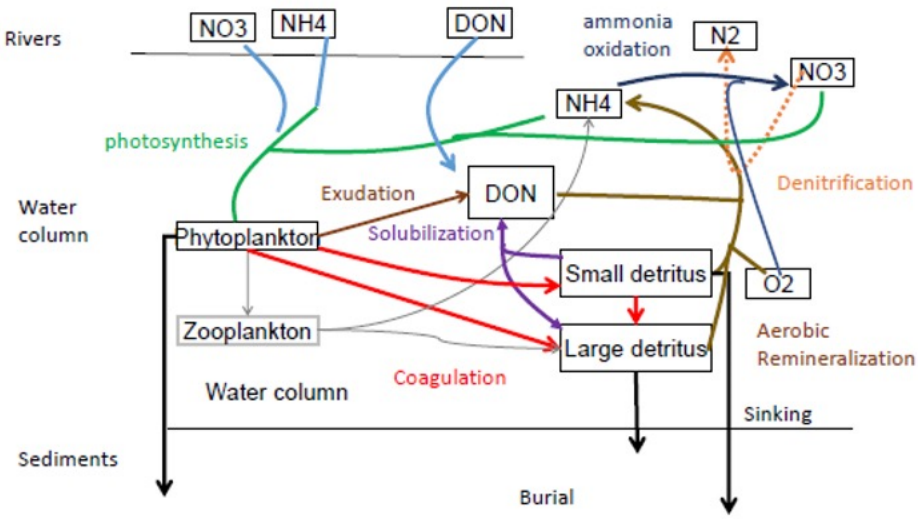

Figure 2. Schematic of biogeochemical nitrogen cycling in the model

The biogeochemical processes incorporated in our model are primarily centered around the nitrogen-based biogeochemical cycle, encompassing various biological interactions and transformations. Figure 2 illustrates the nitrogen cycling process within the water column. Ammonium, nitrate, and dissolved organic nitrogen (DON) are transported to the ocean through river inputs (depicted by light blue lines), and the fluxes of these three components are adopted from a climatology of RIM data from USGS (Zhang and Blomquist, 2018). Subsequently, ammonium and nitrate are assimilated by phytoplankton, whose growth is constrained by both

nitrogen availability and light. A portion of this uptake is associated with zooplankton, while the primary loss mechanism involves the coagulation of phytoplankton into small and large detritus (represented by red lines). Additional loss pathways include sinking to the bottom and exudation of organic matter to DON. An approximate equilibrium can be assumed between the uptake, which depends on the growth rate multiplied by phytoplankton biomass, and the coagulation, which is quadratic in biomass ($\boldsymbol{\mu P \sim \lambda_c P^2}$ where $\boldsymbol{P}$ represents biomass and $\boldsymbol{\lambda_c}$ is the coagulation coefficient). Consequently, the phytoplankton biomass $\boldsymbol{P}$ is roughly proportional to the growth rate. A portion of the detritus undergoes solubilization, resulting in the formation of DON. Both DON and a proportion of the residual detritus undergo remineralization, utilizing oxygen in the presence thereof and denitrification in its absence. The remaining fraction settles to the sediment bed at rates of 0.1 m/day for smaller particles and 5 m/day for larger ones. Upon reaching the sediment bed, it may either be resuspended as smaller detrital particles, the extent of which is contingent upon the degree of bottom turbulence, or undergo burial. The burial fraction ($\boldsymbol{f_{bur}}$) adheres to the model proposed by Henrichs and Reeburgh (1987), wherein it is influenced by the carbon flux reaching the sediment bed.

$$f_{bur} = \min(0.75, 0.023 * carbon\ flux\ to\ the\ bottom^{0.5797}) \quad (1)$$

Consequently, as material flux increases, the burial (fraction*flux) increases even faster. It is worth noting that this implies a positive correlation between local productivity, detritus production, the flux of materials to the sediment bed, and the magnitude of burial. In other words, higher productivity levels result in increased detritus production, subsequently leading to augmented material flux towards the sediment bed and a correspondingly greater quantity being subjected to burial processes.

2.3 Optics in the model

In the Da et al. version of the model, the absorption of PAR is given by an exponential decay, with a diffuse attenuation coefficient k_{PAR} which is a function of space and time. Based on Chesapeake Bay Program data (see Feng et al. 2015) k_{PAR} is described by the equation

$$k_{PAR} = \max(1.4 + 0.063 * TSS - 0.057 * S, 0.6) \quad (2)$$

As already alluded to, the negative dependence on salinity in this equation is a parameterization of the impact of CDOM, which as shown in Fig. 1 is high in the rivers entering the Bay. Note that the Chesroms_ECB code we use does have the ability to include absorption by chlorophyll, but that this is set to zero in the Da et al. (2018) simulations. An alternative formulation (see Feng et al. 2015), provided in the same code, explicitly relates the absorption to refractory DOC delivered down rivers and semilabile DOC that is both delivered down rivers and produced in the Bay.

$$k_{PAR} = 0.04 + 0.0037 * \max(0, DOC - 70.11) + 0.024 * Chl \quad (3)$$

In this study, we employed equation (3), while putting back the effects of total suspended solids (TSS). The formulation is then as follows

$$k_{PAR} = 0.04 + 0.0037 * \max(0, DOC - 70.11) + 0.024 * Chl + 0.063 * TSS \quad (4)$$

By implementing this modification, we achieve a comparable distribution of $\boldsymbol{k_{PAR}}$ as described in equation (2) (Fig. 3, albeit with slightly higher values in mid-Bay and tributaries), enabling us to discern the distinct impacts of refractory DOC and semilabile DOC by activating or deactivating the input of refractory DOC from the riverine source.

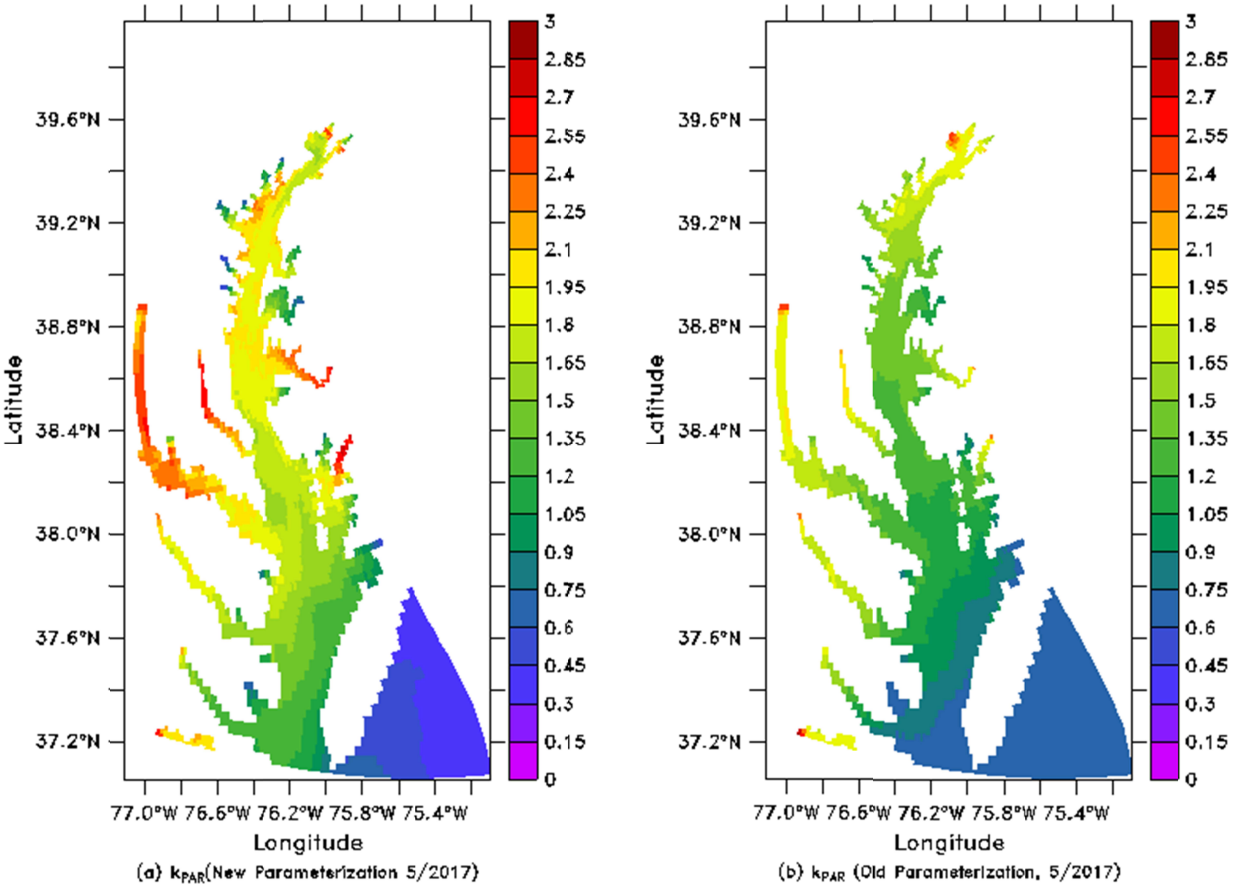

Figure 3. Distribution of k_PAR as described in equation 4 (a) and equation 2 (b)

2.4 Initial conditions and boundary forcings

Riverine inputs for 2015-2018 in the model were obtained from the USGS River Input Monitoring (RIM) Program, as described in Zhang and Blomquist (2018). Tracers such as ISS, NH4, NO3, and DON were assigned identical inputs for various simulations. The seasonal river transport during spring, summer, fall, and winter for 2015, 2016, 2017, and 2018 is depicted in Figure 4. Notably, 2018 exhibited the highest flow rate among the studied years, while 2016 experienced the lowest flow rate.

At the seaward boundary, a combination of radiative boundary conditions and radiation with nudging was applied. This approach allows tracers such as detrital organic matter to exit the domain but prevents their return through the boundary. For temperature and salinity, entering values were set to climatological values. Atmospheric deposition of dissolved inorganic nitrogen (DIN) was also included in the model to account for its significant contribution to the total DIN inputs in the Chesapeake Bay (Da et al., 2018). The simulations were initialized using the initial

conditions of a previously conducted ChesROMS_ECB simulation, which began in 1979 and was run for 38 years. Note that in this simulation inputs of riverine quantities up to 2015 were predicted using the Dynamic Land Ecosystem Model described in Feng et al. (2015) and so exhibit interrelationships between flow and dissolve substances that we do not see in our simulations. However, given the relatively short flushing time of the Bay (~6 months) and the lack of a sediment model in our simulations we do not believe that this change in input parameters affects our basic message.

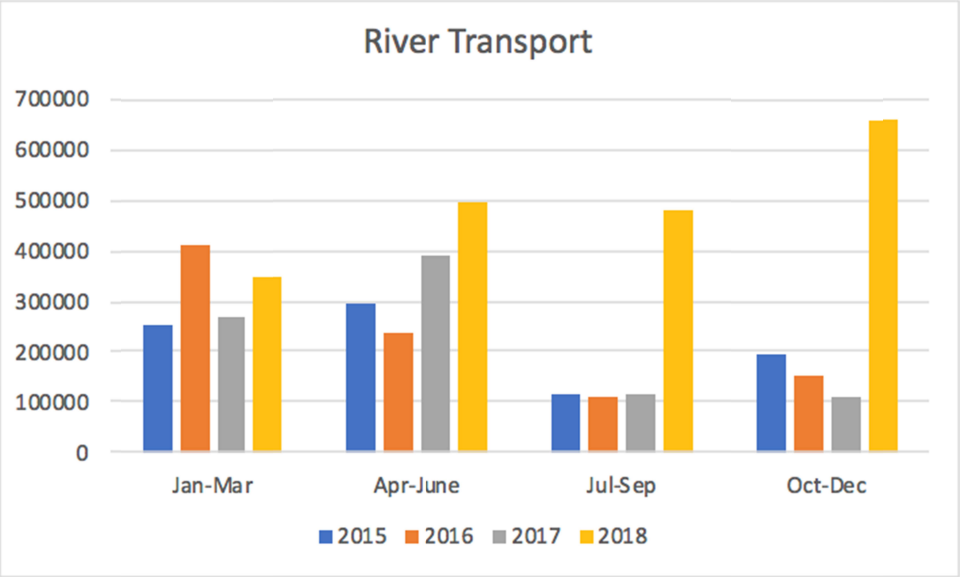

Figure 4. River transport in each season (km^3) (spring, summer, fall and winter) for 2015, 2016, 2017 and 2018 (Multiply by 86400 to get m^3, divide 1e9 to get km^3)

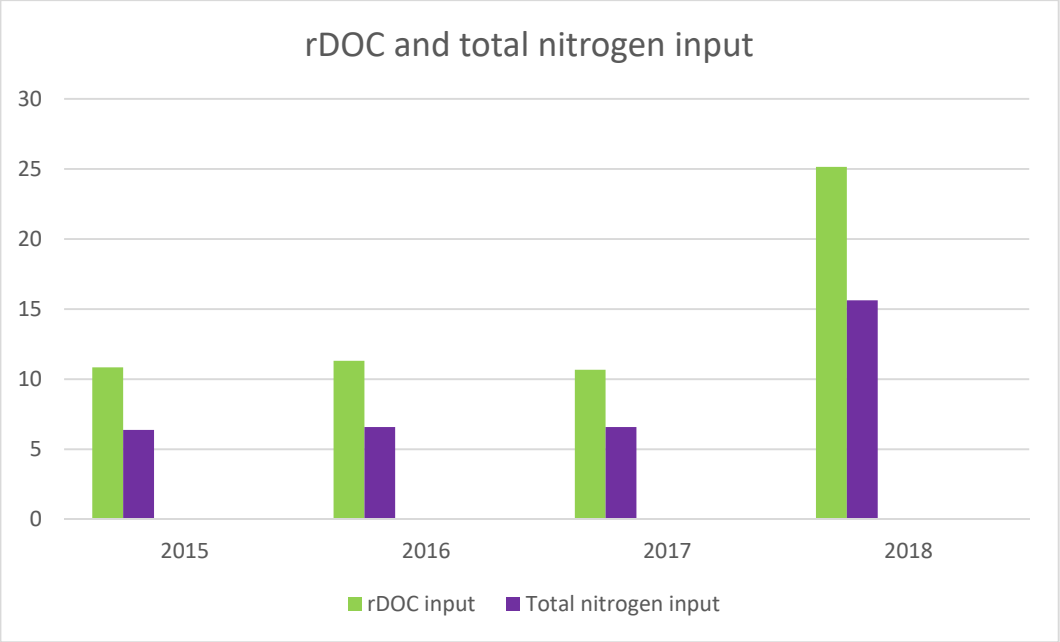

Figure 5. Annually integrated refractory DOC (Gmol C) and total nitrogen input (Gmol N) for 2015, 2016, 2017 and 2018

Figure 5 further illustrates the input of refractory DOC and total nitrogen for all four years. The concentrations of refractory DOC and total nitrogen in riverine systems exhibited consistent levels of input during the years 2015, 2016, and 2017. Despite the presence of seasonal variations in river transport, these variations appeared to mitigate each other when considering the total inputs of refractory DOC and total nitrogen. However, an anomaly was observed in 2018, where the concentrations of refractory DOC and total nitrogen were approximately twice as high as those observed in any of the preceding three years. This discrepancy suggests that the inputs of refractory DOC and total nitrogen may be primarily influenced by riverine inputs occurring between the months of July and September.

3 Results and Discussion

Two simulation runs were conducted spanning the period from 2015 to 2018 to investigate the influence of CDOM associated with riverine refractory DOC. The two runs used distinct riverine inputs, with the control simulation incorporating refractory DOC (control simulation) as measured by USGS and the other run setting the concentration of refractory DOC in river water to zero. This approach enabled a comprehensive comparison of the impact of refractory DOC on the system dynamics and CDOM behavior across multiple years.

3.1 Distribution and intensity of hypoxia

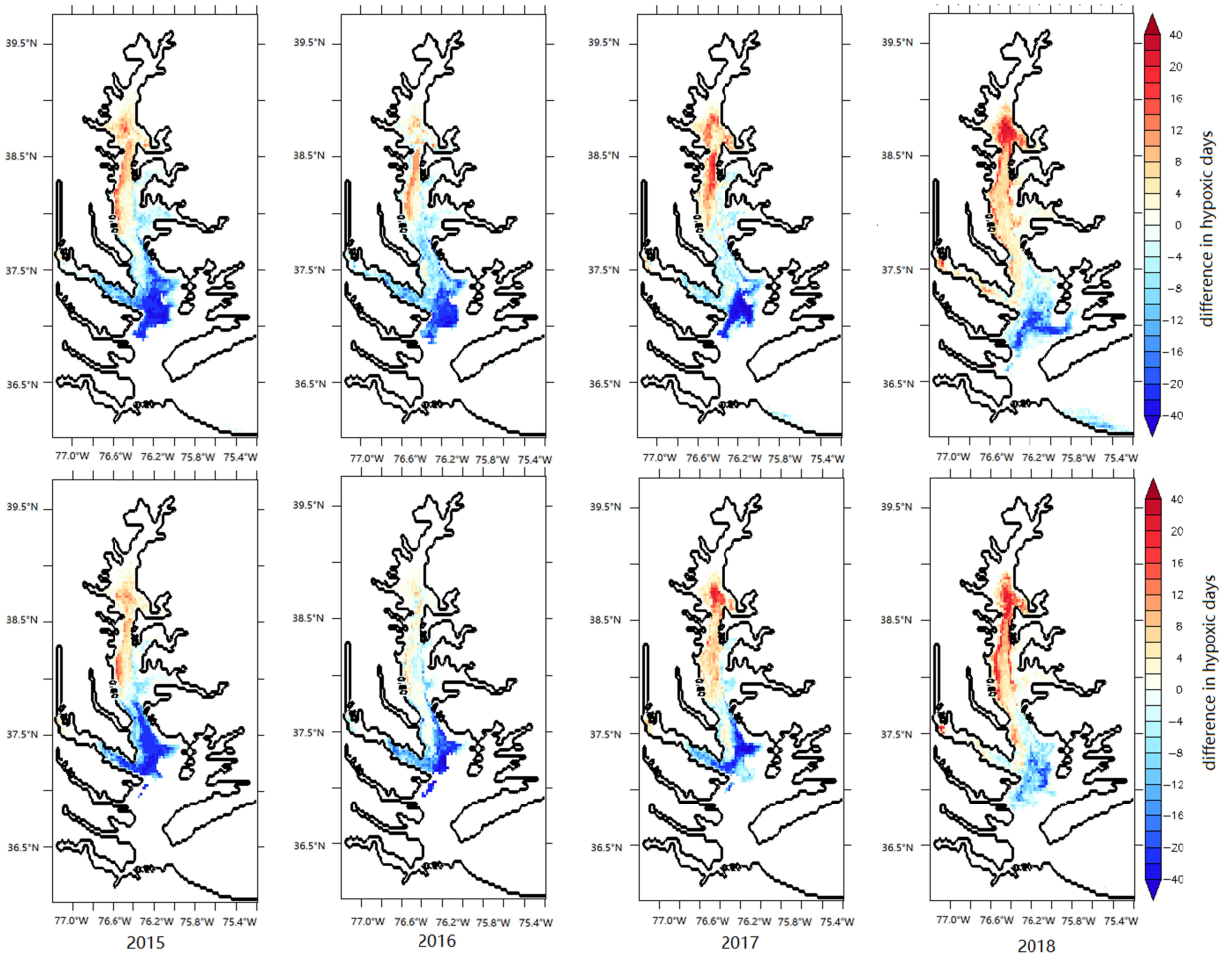

Figure. 6 Upper row: Change in number of days with O_2 <100 mmol/m^3 due to setting refractory DOC to zero for 2015, 2016, 2017 and 2018. Lower row: Change in number of days with O_2 <62.5 mmol/m^3 due to setting refractory DOC to zero for 2015, 2016, 2017 and 2018.

Figure 6 depicts the difference in the number of hypoxic days caused by removing CDOM associated with refractory DOC. Hypoxia is defined as the point at which oxygen concentration drops below 100 mmol/m^3 in the upper panel and below 62.5 mmol/m^3 in the lower panel, as the relevant threshold differs depending on the species of interest. In general, our results indicate that removal of refractory DOC leads to an increase in the duration of hypoxia in the upper bay, but a decrease in the lower bay. The increase in the upper bay is more intensive in 2017 and 2018 than in 2015 and 2016. Varying the threshold for hypoxia does not qualitatively impact the observed outcomes, with both thresholds showing increases in the upper bay and decreases in the lower bay. It is noteworthy that in 2016, the year with the lowest summertime flow and nutrient delivery, when using the lower threshold the removal of refractory DOC predominantly contributes to the reduction of hypoxic conditions. Conversely, in 2018, characterized by high flow rates, CDOM removal slightly amplifies the occurrence of hypoxia.

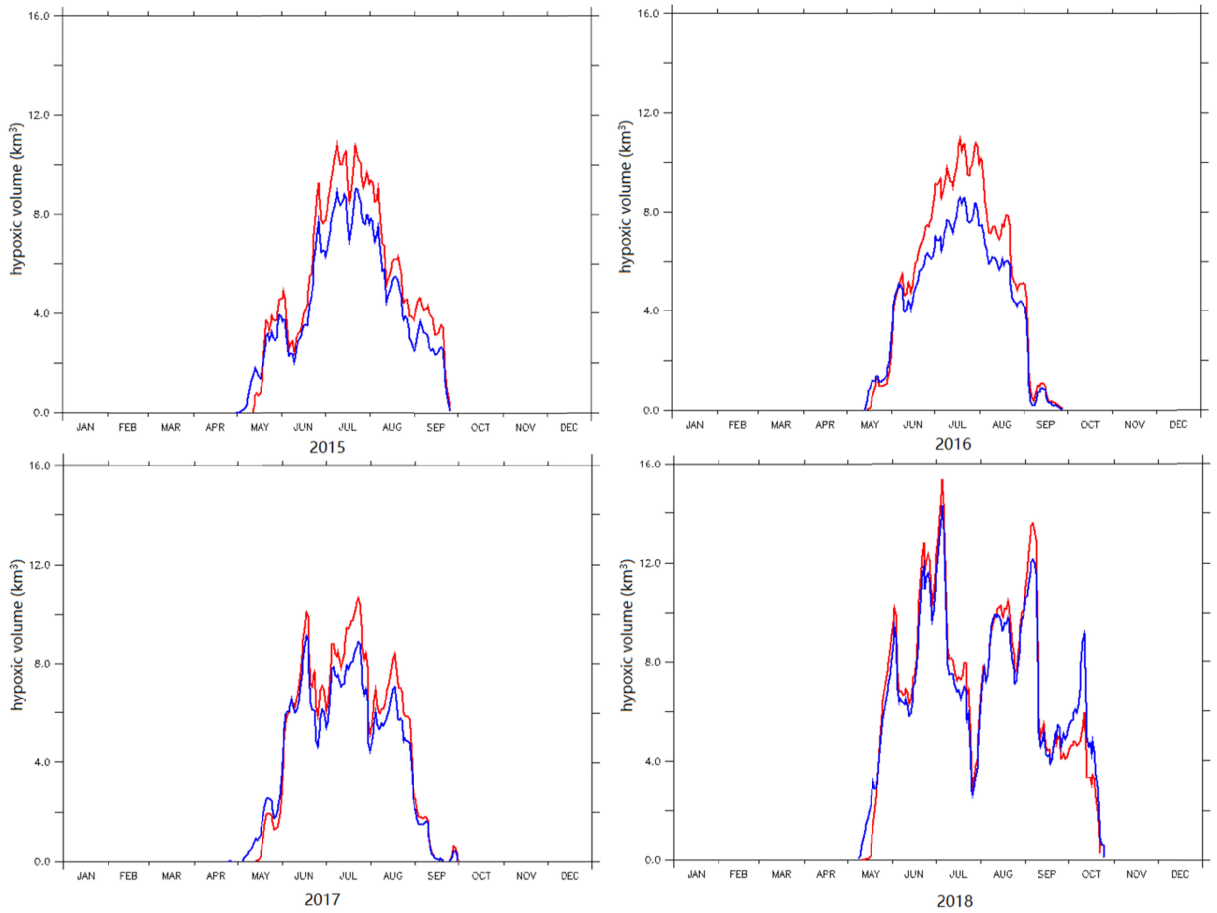

Figure. 7 Hypoxic volume (km^3) for simulation with refractory DOC (red) and without refractory DOC (blue) in 2015, 2016, 2017 and 2018

Figure 7 presents the time series of hypoxic volume across the entire Bay over the course of 2015 to 2018. Our findings demonstrate that removal of refractory DOC leads to a decrease in peak hypoxic volume (indicated by the blue line) compared to the control simulation (red line). However, it also advances the onset of hypoxia for all four years. This effect is evident throughout the time series and supports the conclusion that refractory DOC plays a significant role in the intensity of hypoxia in the Bay. Moreover, compelling evidence indicates that flow dynamics exert a substantial influence on the magnitude of changes resulting from the removal of refractory DOC. In the low-flow year 2016, the removal of refractory DOC leads to an approximate 20% decrease in the overall volume of hypoxia. Conversely, in the high-flow year 2018, the total volume of hypoxia remains relatively unchanged between the two simulations following the removal of refractory DOC.

It is also noteworthy that a notable decline in hypoxic volume occurs around July 26th and 27th, 2018, corresponding to a contraction of the hypoxic zone. This reduction can be attributed to the passage of a storm during those dates, which induced a vigorous mixing event in the southern Bay that propagated northward. The mixing phenomena descends through the water column, facilitated by high winds, resulting in the downward transport of oxygen.

3.2 Dynamics between environmental changes and hypoxia

To further elucidate the factors contributing to changes in hypoxia intensity and distribution resulting from removal of CDOM, we also examined the dynamics of nutrients, detritus, and burial across the two simulation scenarios. Through these analyses, we aimed to investigate the potential links between these factors and observed changes in hypoxia.

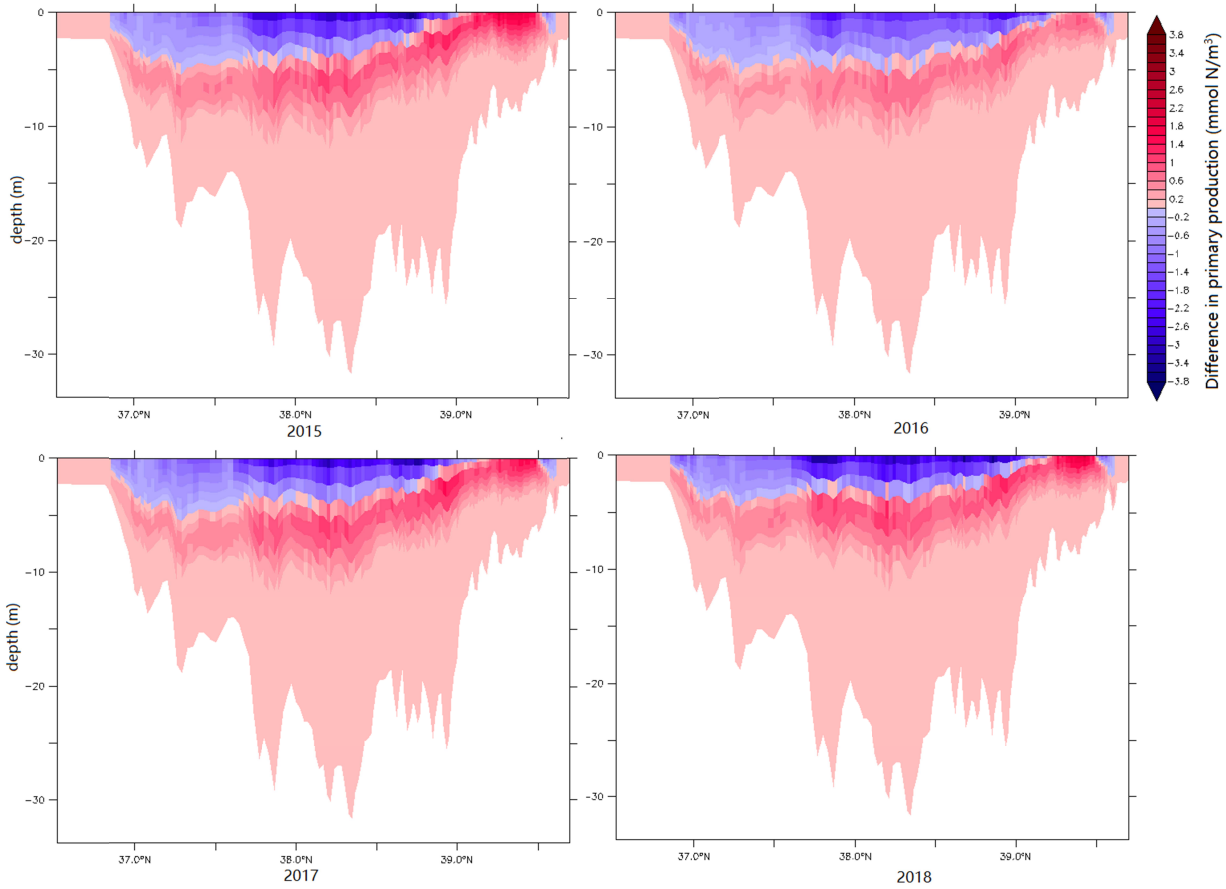

Figure. 8 Primary production differences between simulation without refractory DOC and control simulation for cross section along the mainstem channel of the Bay averaged from June 15th to July 15th in 2015, 2016, 2017 and 2018

Based on our analysis presented in Figure 8, we observe that the impact of CDOM removal on productivity varies across different regions of the Bay. Results for the four years show very similar patterns. In the upper bay, where more light is available due to CDOM removal, we observe an increase in productivity. Conversely, in the middle and lower bay regions, we note a decrease in surface productivity in the simulation without CDOM compared to the control simulation. This is potentially due to a reduction in nutrient availability resulting from greater nutrient utilization in the upper bay. However, our results also reveal an increase in productivity at deeper water depths following CDOM removal, indicating that the availability of light may have been a limiting factor in the control simulation. In a broader context, three distinct signals can be identified. In the upper bay, the location of productivity shifts closer to the surface due to the absence of light limitation. As we move towards the middle bay, productivity increases at greater depths. Additionally, near-surface productivity experiences a decline owing to nutrient

limitations. Overall, these findings suggest that the impact of CDOM on productivity is region-specific and multifaceted, highlighting the need for further investigation into the mechanisms underlying these observations.

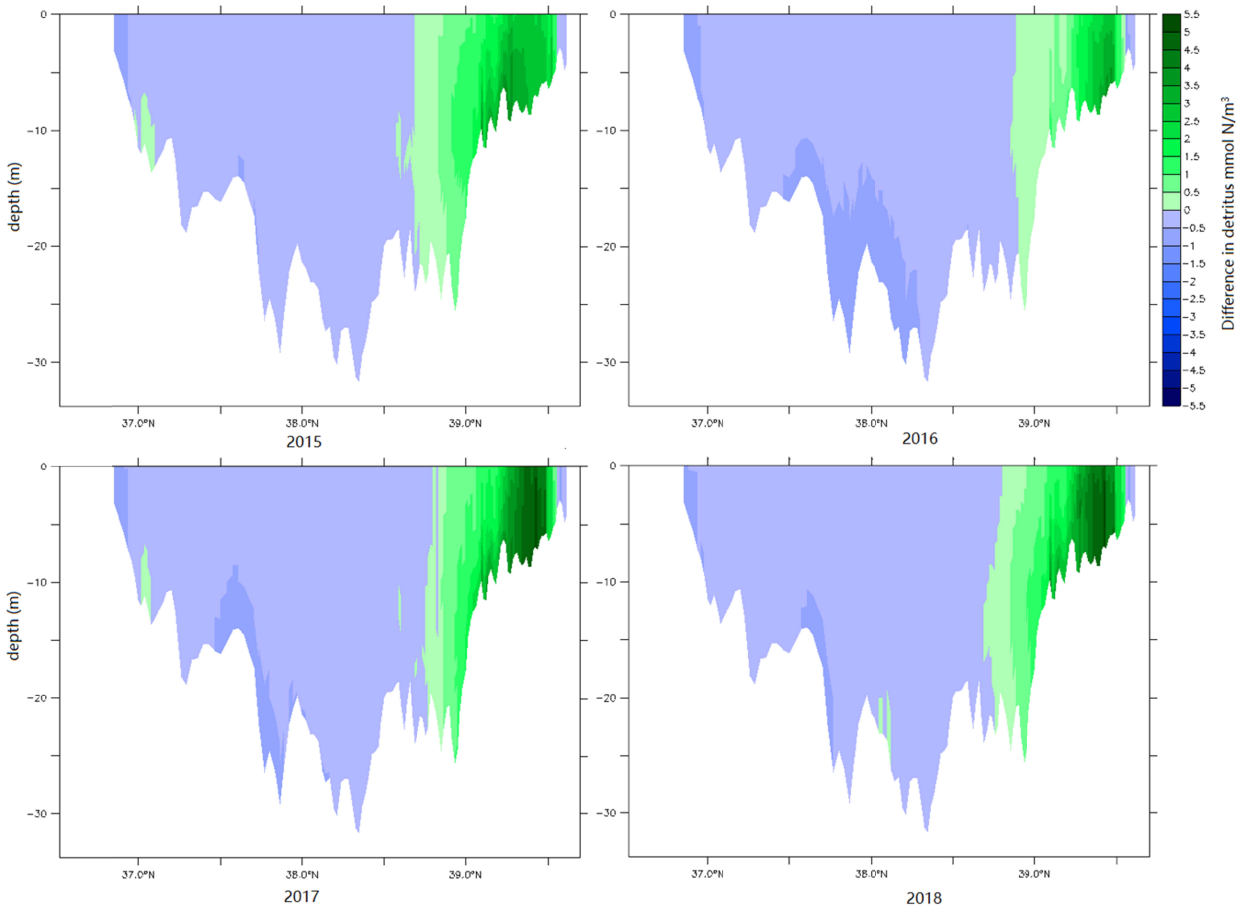

Figure 9. Detritus differences between simulation without refractory DOC and control simulation for cross section along the mainstem channel of the Bay averaged from June 15th to July 15th in 2015, 2016, 2017 and 2018

Our investigation of detritus dynamics (Fig. 9) from four years revealed that removal of CDOM also has varying effects on detritus levels across different regions of the Bay. In the upper bay, we observe an increase in detritus levels following CDOM removal, which is likely due to the elevated productivity levels in this region. However, in the middle and lower bay regions, we note a decrease in detritus levels in the simulation without CDOM compared to the control run, potentially due to the increased remineralization of detrital material at greater depths. It is worth noting that if we were to integrate primary productivity from surface to bottom in these regions, an overall reduction would be seen. Therefore, that could also lead to lower detritus concentrations. These observations underscore the importance of considering both regional and depth-dependent variations in detritus dynamics in order to gain a comprehensive understanding of the factors contributing to changes in hypoxia intensity and distribution.

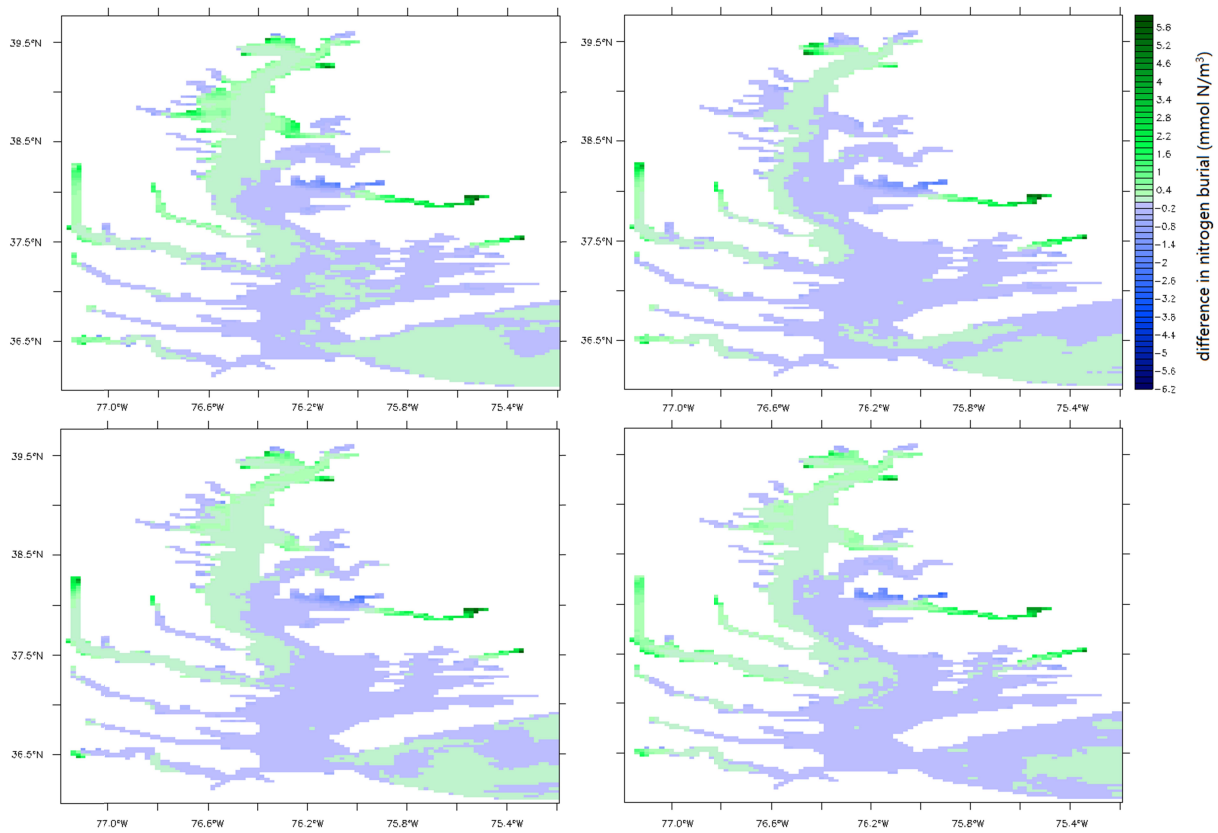

Figure 10. Nitrogen burial differences between simulation without refractory DOC and control simulation across the Bay averaged in July 2015, 2016, 2017 and 2018

An increase in nitrogen burial in the upper bay region can be seen following CDOM removal (Fig. 10), likely due to the elevated production of detritus. In contrast, nitrogen burial levels in the middle and lower bay regions are lower in the simulation without CDOM compared to the control run, which corresponds to decreased detritus levels in the lower bay. Importantly, our findings suggest that the removal of CDOM shifts organic matter remineralization towards the northern regions of the Bay, ultimately resulting in a greater hypoxia intensity in the north compared to the south. These observations highlight the potential for complex and region-specific interactions between environmental factors and hypoxia dynamics in estuarine systems.

	2015	2016	2017	2018
N burial	2.268	2.374	2.502	2.481
N burial (WO)	2.873	2.88	3.132	3.184

Table 1. Comparisons of annually integrated nitrogen burial between simulations with and without refractory DOC for the entire Bay. Values shown are in Gmol.

	2015	2016	2017	2018
denitrification	0.063	0.044	0.063	0.055

denitrification (wo)	0.076	0.049	0.08	0.079
denitrification	1.442	1.365	1.553	2.383
denitrification (wo)	1.273	1.177	1.419	2.379

Table 2. Comparisons of annually integrated water column denitrification between simulations with and without refractory DOC: Head of the Bay (Upper) vs. Other parts of the Bay (Lower). Values shown are in Gmol.

Table 2 and Table 1 provide a comprehensive overview of the changes observed in the nitrogen budget for the Bay when refractory DOC is removed. On a broader scale, the nitrogen burial for the entire Bay exhibits an overall increase following the removal of refractory DOC. However, upon closer examination of specific regions within the Bay, notable variations are observed. In the main channel of the Bay, we observe an increase in nitrogen burial in the upper Bay, while a decrease in burial is evident when moving towards the middle and lower Bay regions as shown in Fig. 10. Moreover, within the estuaries, a significant increase in nitrogen burial is observed. We get an about 30% increase in burial, but this is partially offset by a decrease in main stem of the Bay.

To gain further insights into the processes at play, we divided water column denitrification into two distinct regions: the head of the Bay (north of 39.0 N°) and the other parts of the Bay. Corresponding to the findings depicted in Fig. 9, when removing refractory DOC, we observe a higher magnitude of both burial and denitrification at the head of the Bay. However, as we move towards the middle and lower Bay regions, there is a gradual reduction in both burial and denitrification rates. These results indicate that limiting the input of refractory DOC leads to increased burial of nitrogen at the rivers, with variations observed across different parts of the Bay and the water column.

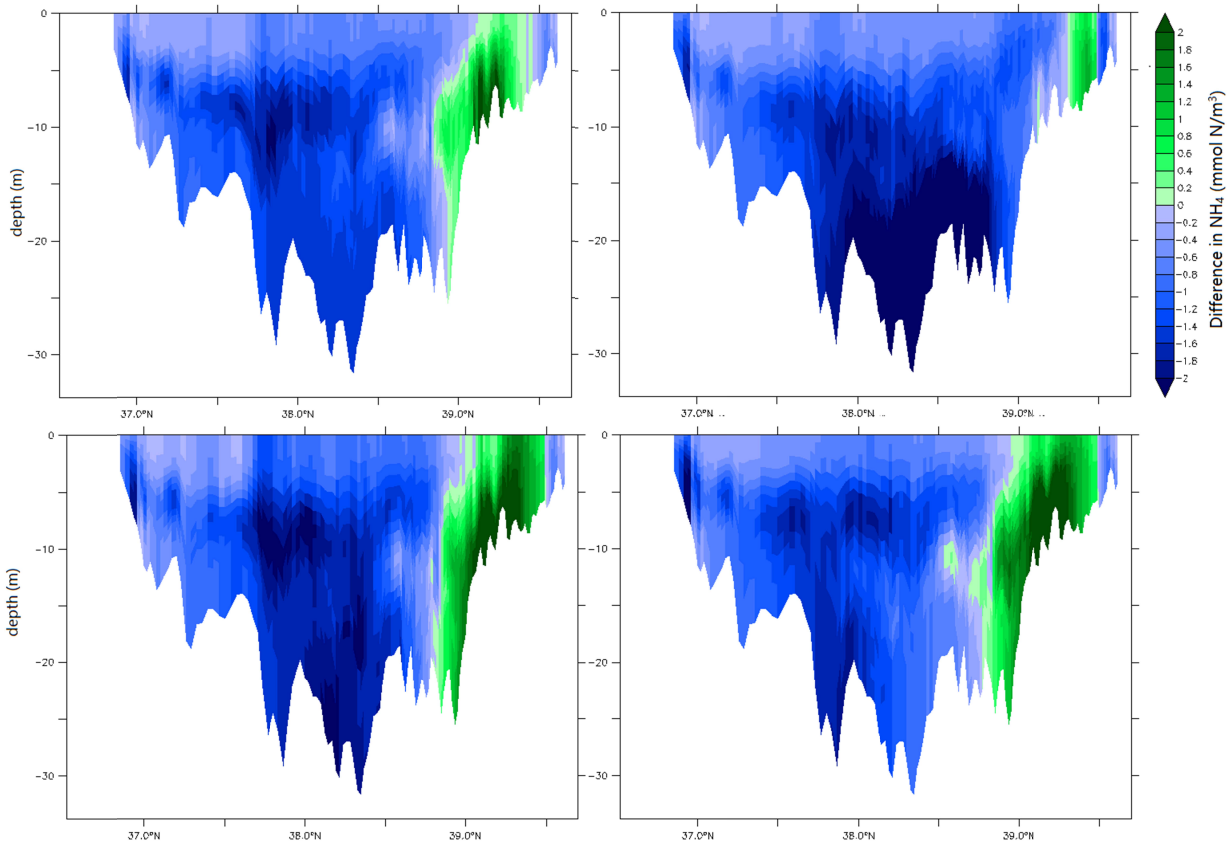

Figure.11 Ammonium differences between simulation without refractory DOC and control simulation for cross section along the mainstem channel of the Bay averaged from June 15th to July 15th in 2015, 2016, 2017 and 2018

Regarding ammonium dynamics (Fig. 11), we observe an increase in ammonium levels in the upper bay following CDOM removal, which may be attributed to higher productivity levels leading to increased respiration. Notably, the specific regions experiencing an augmentation in ammonium concentrations vary across different years, with 2018 exhibiting the most extensive increment and 2016 displaying the smallest magnitude of change. In the case of 2016, the ammonium regeneration in the upper bay is found to be minimal. This observation can be attributed to the lower flow conditions, which limited the supply of ammonium and consequently led to a faster depletion of NH_4. As a result, the remineralization of NH_4 in the upper bay was reduced, and the impact of CDOM removal was primarily confined to this shallow region. However, in both 2017 and 2018, the hypoxic event expanded beyond the upper bay, encompassing the middle and lower bay regions. This expansion resulted in more pronounced declines in oxygen levels compared to 2016.

In contrast, in the middle and lower bay regions, we noted a decrease in ammonium levels due to refractory DOC removal, potentially due to the utilization of ammonium as a nutrient source by the increased productivity in these regions. The reduction in integrated primary production also contributes to decreased ammonium levels by leading to a decline in detritus. These observations highlight the complex interplay between nutrient dynamics, circulation and productivity levels.

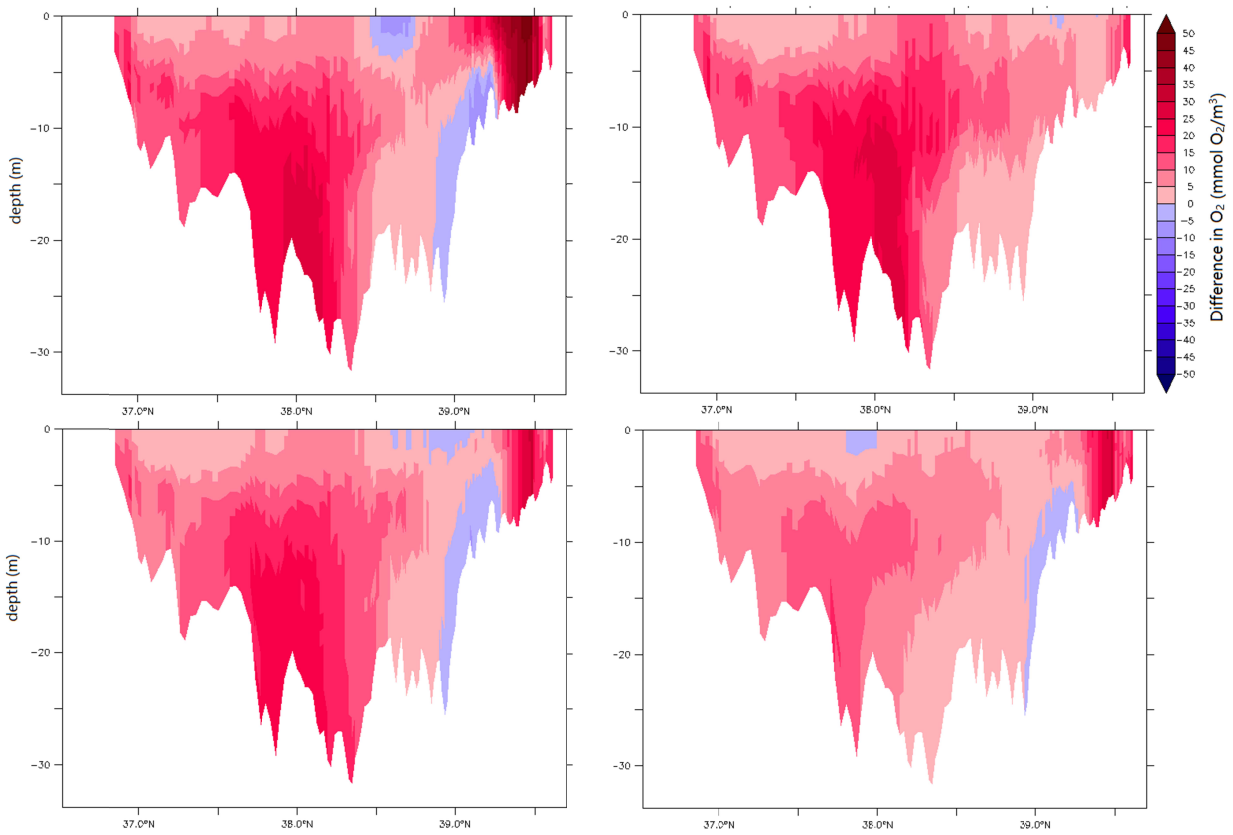

Figure 12. Oxygen differences between simulation without refractory DOC and control simulation for cross section along the mainstem channel of the Bay averaged from June 15th to July 15th in 2015, 2016, 2017 and 2018

The observed alterations in oxygen levels align with the changes in ammonium concentrations, as illustrated in Figure 12. In the upper bay there is a notable increase in oxygen concentrations, potentially attributable to enhanced productivity subsequent to CDOM removal. However, as we transition towards the middle bay, a decline in surface oxygen concentration becomes apparent, along with decreased oxygen levels in deeper sections of the water column in certain areas. These reductions are likely a consequence of elevated rates of remineralization.

In the lower Bay, we observe a subsequent increase in oxygen levels, attributed to the removal of CDOM as remineralization processes become less pronounced.

It is worth noting that the extent of the oxygen-depleted zone exhibits variations among different years, with 2018 displaying the largest area of oxygen decline, while 2016 represents the smallest region affected. Importantly, these trends correspond to the respective zones of changes in ammonium concentrations.

4 Conclusions and future work

Previous studies have focused on examining the influence of Colored Dissolved Organic Matter (CDOM) on optical properties. However, the parameterization of CDOM absorption in these studies did not explicitly include CDOM, which subsequently limited the exploration of its

436 impacts in subsequent models. In our research, we address this limitation by employing a more
437 accurate representation of CDOM absorption specifically tailored for the Chesapeake Bay.
438 Through a series of experiments, we investigated the intricate dynamics between CDOM and
439 coastal ocean hypoxia, allowing for a comprehensive comparison of the effects of refractory
440 Dissolved Organic Carbon (DOC) on system dynamics and CDOM behavior across multiple
441 years. Our findings highlight that the impact of CDOM on nutrient dynamics and productivity is
442 highly dependent on the region and exhibits multifaceted characteristics. Furthermore, we
443 observed that the removal of refractory DOC is significantly influenced by flow dynamics,
444 resulting in varying magnitudes of changes in the system.

445 So far, our findings indicate that refractory DOC input is a major contributor to the overall
446 hypoxia levels in both the lower Bay and tributaries, although the specific impacts of CDOM
447 associated with refractory DOC on hypoxia dynamics may differ between these regions since the
448 impact of CDOM on nutrient dynamics and productivity varies significantly across different
449 parts of Chesapeake Bay. In the upper Bay, the mitigation of CDOM leads to a reduction in light
450 limitation, thereby fostering heightened primary productivity. Consequently, this heightened
451 productivity gives rise to increased detritus production and subsequent burial processes, thereby
452 contributing to elevated hypoxia levels. Conversely, as we move towards the middle and lower
453 reaches of the Bay, CDOM mitigation can induce a decline in integrated primary productivity
454 due to nutrient absorption occurring primarily in the upper Bay. This reduction in productivity is
455 concomitant with diminished burial and denitrification processes, ultimately resulting in a
456 decrement in hypoxia levels. Therefore, future research should aim to elucidate the relative
457 importance of refractory DOC and associated CDOM in driving hypoxia intensity and
458 distribution across the main stem of the Bay versus tributary systems.

459 Additionally, our investigation highlights the potential for streamflow and mixing to drive
460 significant variability in hypoxic volume over time. As such, it will be crucial to evaluate the
461 impact of changing environmental conditions and inter-annual variability on hypoxia dynamics
462 to gain a more comprehensive understanding of the underlying mechanisms driving these
463 dynamics. Ultimately, such efforts will be essential for developing effective strategies for
464 mitigating and managing hypoxia in the Chesapeake Bay and other estuarine systems facing
465 similar challenges.

466 An additional concern that warrants attention in this study is the assumption made regarding the
467 independence of CDOM concentration and composition (50% of DOC is assumed to be
468 refractory) from flow rate. Additionally, the compostion is the same for all rivers. It is important
469 to acknowledge that future iterations of this research should consider both flow rate and land use
470 partterns, as there is evidence that both of these influce the concentration and composition of
471 CDOM (S. Kaushal, pers. Comm.).

472 The observed findings also raise a pertinent question regarding the inclusion of refractory DOC
473 management in estuary management practices. It becomes crucial to consider whether the
474 removal of DOC is a viable strategy, particularly when applied to estuaries of varying sizes. For
475 smaller estuaries, the removal of DOC could potentially yield positive outcomes. However, in
476 the context of larger estuaries, such a strategy may not be as beneficial.

477

Data Availability Statement

Data will be available on Zenodo. Codes can be access from ROMS repository.

References

Aksnes, D., Dupont, N., Staby, A., Fiksen, Ø., Kaartvedt, S., & Aure, J. (2009). Coastal water darkening and implications for mesopelagic regime shifts in Norwegian fjords. Marine Ecology Progress Series, 387, 39–49. https://doi.org/10.3354/meps08120

Balch, W., Huntington, T., Aiken, G., Drapeau, D., Bowler, B., Lubelczyk, L., & Butler, K. (2016). Toward a quantitative and empirical dissolved organic carbon budget for the Gulf of Maine, a semienclosed shelf sea. Global Biogeochemical Cycles, 30(2), 268–292. https://doi.org/10.1002/2015GB005332

Brothers, S., Köhler, J., Attermeyer, K., Grossart, H. P., Mehner, T., Meyer, N., et al. (2014). A feedback loop links brownification and anoxia in a temperate, shallow lake. Limnology and Oceanography, 59(4), 1388–1398. https://doi.org/10.4319/lo.2014.59.4.1388

Brown, C. W., Hood, R. R., Long, W., Jacobs, J., Ramers, D. L., Wazniak, C., et al. (2013). Ecological forecasting in Chesapeake Bay: Using a mechanistic–empirical modeling approach. Journal of Marine Systems, 125, 113–125. https://doi.org/10.1016/j.jmarsys.2012.12.007

Cao, F., Tzortziou, M., Hu, C., Mannino, A., Fichot, C. G., Del Vecchio, R., et al. (2018). Remote sensing retrievals of colored dissolved organic matter and dissolved organic carbon dynamics in North American estuaries and their margins. Remote Sensing of Environment, 205, 151–165. https://doi.org/10.1016/j.rse.2017.11.014

Cao, J., Sun, Q., Zhao, D., Xu, M., Shen, Q., Wang, D., et al. (2020). A critical review of the appearance of black-odorous waterbodies in China and treatment methods. Journal of Hazardous Materials, 385, 121511. https://doi.org/10.1016/j.jhazmat.2019.121511

Cerco, C. F., & Noel, M. R. (2017). The 2017 Chesapeake Bay water quality and sediment transport model. Retrieved from https://www.chesapeake.org/stac/presentations/277_20170501_Cerco and Noel 2017_WQSTM Draft Report.pdf

Da, F., Friedrichs, M. A. M., & St-Laurent, P. (2018). Impacts of Atmospheric Nitrogen Deposition and Coastal Nitrogen Fluxes on Oxygen Concentrations in Chesapeake Bay. Journal of Geophysical Research: Oceans, 123(7), 5004–5025. https://doi.org/10.1029/2018JC014009

Diaz, R. J., & Rosenberg, R. (2008). Spreading Dead Zones and Consequences for Marine Ecosystems. Science, 321(5891), 926–929. https://doi.org/10.1126/science.1156401

Estlander, S., Pippingsköld, E., & Horppila, J. (2021). Artificial ditching of catchments and brownification-connected water quality parameters of lakes. Water Research, 205, 117674. https://doi.org/10.1016/j.watres.2021.117674

Feng, Y., Friedrichs, M. A. M., Wilkin, J., Tian, H., Yang, Q., Hofmann, E. E., et al. (2015). Chesapeake Bay nitrogen fluxes derived from a land-estuarine ocean biogeochemical modeling

system: Model description, evaluation, and nitrogen budgets. Journal of Geophysical Research: Biogeosciences, 120(8), 1666–1695. https://doi.org/10.1002/2015JG002931

Fennel, K., & Testa, J. M. (2019). Biogeochemical Controls on Coastal Hypoxia. Annual Review of Marine Science, 11(1), 105–130. https://doi.org/10.1146/annurev-marine-010318-095138

Gallegos, C. L. (2001). Calculating Optical Water Quality Targets to Restore and Protect Submersed Aquatic Vegetation: Overcoming Problems in Partitioning the Diffuse Attenuation Coefficient for Photosynthetically Active Radiation. Estuaries, 24(3), 381. https://doi.org/10.2307/1353240

Gnanadesikan, A., Kim, G. E., & Pradal, M. S. (2019). Impact of Colored Dissolved Materials on the Annual Cycle of Sea Surface Temperature: Potential Implications for Extreme Ocean Temperatures. Geophysical Research Letters, 46(2), 861–869. https://doi.org/10.1029/2018GL080695

Green, S. A., & Blough, N. V. (1994). Optical absorption and fluorescence properties of chromophoric dissolved organic matter in natural waters. Limnology and Oceanography, 39(8), 1903–1916. https://doi.org/10.4319/lo.1994.39.8.1903

Henrichs, S. M., & Reeburgh, W. S. (1987). Anaerobic mineralization of marine sediment organic matter: Rates and the role of anaerobic processes in the oceanic carbon economy. Geomicrobiology Journal, 5(3–4), 191–237. https://doi.org/10.1080/01490458709385971

Jin, R., Pradal, M.-A., Hantsoo, K., Gnanadesikan, A., St-Laurent, P., & Bjerrum, C. J. (2023a). Comparing two ocean biogeochemical models of Chesapeake Bay with and without the sulfur cycle instead highlights the importance of particle sinking, burial, organic matter, nitrification and light attenuation. Ocean Modelling, 182, 102175. https://doi.org/10.1016/j.ocemod.2023.102175

Jin, R., Pradal, M.-A., Hantsoo, K., Gnanadesikan, A., St-Laurent, P., & Bjerrum, C. J. (2023b). Constructing a model including the cryptic sulfur cycle in Chesapeake Bay requires judicious choices for key processes and parameters. MethodsX, 11, 102253. https://doi.org/10.1016/j.mex.2023.102253

Kahru, M., Bittig, H., Elmgren, R., Fleming, V., Lee, Z., & Rehder, G. (2022). Baltic Sea transparency from ships and satellites: centennial trends. Marine Ecology Progress Series, 697, 1–13. https://doi.org/10.3354/meps14151

Kemp, W., Boynton, W., Adolf, J., Boesch, D., Boicourt, W., Brush, G., et al. (2005). Eutrophication of Chesapeake Bay: historical trends and ecological interactions. Marine Ecology Progress Series, 303, 1–29. https://doi.org/10.3354/meps303001

Kim, G. E., Pradal, M.-A., & Gnanadesikan, A. (2015). Quantifying the biological impact of surface ocean light attenuation by colored detrital matter in an ESM using a new optical parameterization. Biogeosciences, 12(16), 5119–5132. https://doi.org/10.5194/bg-12-5119-2015

Kim, Grace E., Gnanadesikan, A., & Pradal, M.-A. (2016). Increased Surface Ocean Heating by Colored Detrital Matter (CDM) Linked to Greater Northern Hemisphere Ice Formation in the GFDL CM2Mc ESM. Journal of Climate, 29(24), 9063–9076. https://doi.org/10.1175/JCLI-D-16-0053.1

Kim, Grace E., St-Laurent, P., Friedrichs, M. A. M., & Mannino, A. (2020). Impacts of Water Clarity Variability on Temperature and Biogeochemistry in the Chesapeake Bay. Estuaries and Coasts, 43(8), 1973–1991. https://doi.org/10.1007/s12237-020-00760-x

Knoll, L. B., Williamson, C. E., Pilla, R. M., Leach, T. H., Brentrup, J. A., & Fisher, T. J. (2018). Browning-related oxygen depletion in an oligotrophic lake. Inland Waters, 8(3), 255–263. https://doi.org/10.1080/20442041.2018.1452355

Kritzberg, E. S., Hasselquist, E. M., Škerlep, M., Löfgren, S., Olsson, O., Stadmark, J., et al. (2020). Browning of freshwaters: Consequences to ecosystem services, underlying drivers, and potential mitigation measures. Ambio, 49(2), 375–390. https://doi.org/10.1007/s13280-019-01227-5

Luettich, R. A., Westerink, J. J., & Scheffner, N. W. (1992). ADCIRC: an advanced three-dimensional circulation model for shelves, coasts, and estuaries. Report 1, Theory and methodology of ADCIRC-2DD1 and ADCIRC-3DL. Retrieved from https://hdl.handle.net/11681/4618

Luther, G. W., & Church, T. M. (1988). Seasonal cycling of sulfur and iron in porewaters of a Delaware salt marsh. Marine Chemistry, 23(3–4), 295–309. https://doi.org/10.1016/0304-4203(88)90100-4

Mesinger, F., DiMego, G., Kalnay, E., Mitchell, K., Shafran, P. C., Ebisuzaki, W., et al. (2006). North American Regional Reanalysis. Bulletin of the American Meteorological Society, 87(3), 343–360. https://doi.org/10.1175/BAMS-87-3-343

Miller, R. L., Belz, M., Castillo, C. Del, & Trzaska, R. (2002). Determining CDOM absorption spectra in diverse coastal environments using a multiple pathlength, liquid core waveguide system. Continental Shelf Research, 22(9), 1301–1310. https://doi.org/10.1016/S0278-4343(02)00009-2

Monteith, D. T., Stoddard, J. L., Evans, C. D., de Wit, H. A., Forsius, M., Høgåsen, T., et al. (2007). Dissolved organic carbon trends resulting from changes in atmospheric deposition chemistry. Nature, 450(7169), 537–540. https://doi.org/10.1038/nature06316

Rabalais, N. N., Turner, R. E., Díaz, R. J., & Justić, D. (2009). Global change and eutrophication of coastal waters. ICES Journal of Marine Science, 66(7), 1528–1537. https://doi.org/10.1093/icesjms/fsp047

Scavia, D., Kelly, E. L. A., & Hagy, J. D. (2006). A simple model for forecasting the effects of nitrogen loads on Chesapeake Bay hypoxia. Estuaries and Coasts, 29(4), 674–684. https://doi.org/10.1007/BF02784292

Scully, M. E. (2016). The contribution of physical processes to inter-annual variations of hypoxia in Chesapeake Bay: A 30-yr modeling study. Limnology and Oceanography, 61(6), 2243–2260. https://doi.org/10.1002/lno.10372

Shchepetkin, A. F., & McWilliams, J. C. (2005). The regional oceanic modeling system (ROMS): a split-explicit, free-surface, topography-following-coordinate oceanic model. Ocean Modelling, 9(4), 347–404. https://doi.org/10.1016/j.ocemod.2004.08.002

Siegel, D. A. (2005). Colored dissolved organic matter and its influence on the satellite-based characterization of the ocean biosphere. Geophysical Research Letters, 32(20), L20605. https://doi.org/10.1029/2005GL024310

STANLEY, E. H., POWERS, S. M., LOTTIG, N. R., BUFFAM, I., & CRAWFORD, J. T. (2012). Contemporary changes in dissolved organic carbon (DOC) in human-dominated rivers: is there a role for DOC management? Freshwater Biology, 57, 26–42. https://doi.org/10.1111/j.1365-2427.2011.02613.x

Steffen, W., Crutzen, P. J., & McNeill, J. R. (2020). 2. The Anthropocene. In Environment and Society (pp. 12–31). New York University Press. https://doi.org/10.18574/nyu/9781479844746.003.0006

Virginia Institute of Marine Sciences. (2023). Real-time estimates of hypoxic water. Retrieved from https://www.vims.edu/research/products/cbefs/hypoxic-volume/index.php

de Wit, H. A., Stoddard, J. L., Monteith, D. T., Sample, J. E., Austnes, K., Couture, S., et al. (2021). Cleaner air reveals growing influence of climate on dissolved organic carbon trends in northern headwaters. Environmental Research Letters, 16(10), 104009. https://doi.org/10.1088/1748-9326/ac2526

Yamashita, Y., Nosaka, Y., Suzuki, K., Ogawa, H., Takahashi, K., & Saito, H. (2013). Photobleaching as a factor controlling spectral characteristics of chromophoric dissolved organic matter in open ocean. Biogeosciences, 10(11), 7207–7217. https://doi.org/10.5194/bg-10-7207-2013

Yamashita, Youhei, & Tanoue, E. (2008). Production of bio-refractory fluorescent dissolved organic matter in the ocean interior. Nature Geoscience, 1(9), 579–582. https://doi.org/10.1038/ngeo279

Zhang, Q., & Blomquist, J. D. (2018). Watershed export of fine sediment, organic carbon, and chlorophyll-a to Chesapeake Bay: Spatial and temporal patterns in 1984–2016. Science of The Total Environment, 619–620, 1066–1078. https://doi.org/10.1016/j.scitotenv.2017.10.279